

11-22-92

132911

20p

HIGH SPEED TRANSITION PREDICTION

Gediminas Gasperas

(NASA-CR-194125) HIGH SPEED
TRANSITION PREDICTION Final Report
(MCAT Inst.) 20 p

N94-13422

Unclas

G3/02 0182911

August 1993

NCC2-704

MCAT Institute
3933 Blue Gum Drive
San Jose, CA 95127

HIGH SPEED TRANSITION PREDICTION

Gediminis Gasperas

Introduction:

The main objective of this work period was to develop, maintain and exercise, state-of-the-art methods for transition prediction in supersonic flowfields. Basic state and stability codes, acquired during the last work period, were exercised and applied to calculate the properties of various flowfields. The development of a code for the prediction of transition location using a currently novel method (the PSE or Parabolized Stability Equation method), initiated during the last work period and continued during the present work period, was cancelled at mid-year for budgetary reasons.

Other activities during this period included the presentation of a paper at the APS meeting in Tallahassee, Florida entitled "Stability of Two-Dimensional Compressible Boundary Layers", as well as the initiation of a paper co-authored with H. Reed of the Arizona State University entitled "Stability of Boundary Layers".

a) 3-D Boundary Layer Code

A 3-D boundary layer code written by J.E. Harris of NASA Langley and V. Iyer of Vigyan Research Associates in Hampton, Virginia (Ref. 1) was acquired during the previous work period (Ref. 2). The code is fourth-order accurate and is applicable to compressible flow on wings and fuselages, as well as to other geometries. The code was to be used in an attempt to overcome the limitations inherent in the Kaups and Cebeci code using the conical flow assumption, and which is coupled to the COSAL stability code (Ref.3). As mentioned in Ref. 2, other versions of the code were to be acquired from the author as soon as they were completed. These included versions applicable to swept wings in orthogonal coordinates, general swept wings, and a Navier-Stokes to COSAL interface.

The latter activity, the Navier-Stokes to COSAL interface, became the domain of L. King of FML, while the other versions of the code were not received from V. Iyer, presumably because they are not yet completed because of other commitments.

After activity on the PSE code development was stopped, more activity was concentrated on attempting to use the 3D code to solve cases of particular interest at the FML. Accordingly, all the ten test cases provided in Ref.1 were run to ensure proper functioning of the code. The most relevant test case to the FML was Case 10, which is the Mach 0.5 flow over a swept wing on non-tapered cross section of a NACA 0012 airfoil. As it is mentioned in Ref. 1, the 3D code is said to be applicable to not only swept but also swept and tapered, as well as swept and cranked wings (Ref.1, p.141). Since the case of immediate current interest at the FML was a swept and tapered NACA 64A010 airfoil at Mach 1.5, Case 10 was of the most immediate interest, being closest to the case of interest at the FML, and was therefore studied in detail.

Test Case 10 was studied in detail with the object of preparing a short summary on how to run the 3D boundary layer code. This was to help others at NASA Ames and the FML who might be interested later in using the code. Because problems arose in applying the 3D code with locally generated inviscid inputs, the summary consists of the notes that follow here. In addition to these notes, J. Garcia of NASA Ames was instructed in the running of the code, and made copies of all relevant computer files and directories involved in the running of the code. Also, the author would be available in the future for voluntary occasional assistance should the need arise, currently having the most experience in using the code at NASA Ames.

The 3D boundary layer code was to be used for the prediction of the boundary layer over a swept and tapered NACA 64A010 airfoil at Mach 1.5. Local Euler solutions, generated by E. Tu and J. Garcia of NASA Ames were to be used as input conditions. However, the boundary layer code did not run with the locally generated inputs. It was eventually determined that the results which were output from the attachment line relocation program in the 3D code were incorrect for the NACA 64A010 inputs. What follows are comparisons from running Test Case 10 for the NACA 0012, and from running the tapered NACA 64A010 airfoil. The purpose is to show where the difficulties occur in the program in the event it is desired to have the code working for locally generated inputs. In particular, the purpose of this exercise is to provide a review of the last instruction session with J. Garcia. This will be useful in the event that he becomes responsible for the code at Ames at a future date.

Figures 1 to 4 are shown to define the geometries of the airfoils of interest. Figure 1 shows selected cross sections of the NACA 0012 and Figure 2 shows selected cross sections of the NACA 64A010. As can be seen in the figures, the NACA 0012 airfoil has constant cross sections. Because the airfoil is swept, the X-origin is seen as increasing. The NACA 64A010 airfoil is both swept and tapered. Although the cross sections originate at larger X-values out towards the tip, the cross section profiles decrease as well.

Figure 3 is a plan view of various span stations for the NACA 0012 airfoil. As can be seen, the span stations are of constant length, and are merely displaced in X because of the sweep. Figure 4, however, is a plan view of selected stations of the NACA 64A010. In addition to having the leading edges displaced in X, the span stations continue to shrink in length, ie. they are of non-constant chord. The trailing edge is always at an X of 1.0.

As has been mentioned earlier, Test Case 10, provided with the 3D boundary layer code, was found to run with no difficulties using the inputs provided by the source. These inputs are here to be compared with the inputs provided locally to see if the locally supplied inputs have any drastically different features, an event which may be a clue to the source of the difficulties. Figure 5 shows selected C_p plots for various span stations for the NACA 0012. Since the geometric cross sections are the same, it is to be expected that the C_p distributions would be rather similar, and such is indeed the case. Also, as is typical of a non-laminar flow airfoil, the suction peak occurs very close to the leading edge, with a gradual suction decrease which continues out to the vicinity of the trailing edge. Figure 6 shows C_p distributions for selected span stations for the tapered NACA 64A010 airfoil. As is typical for airfoils which attempt to maintain a longer run of laminar flow, the suction peak is achieved only near the trailing edge, with a rather abrupt increase in pressure afterwards. It is again to be noted that these solutions were locally generated, and that

these were the solutions with which difficulties were encountered. Nothing unusual however, is immediately apparent in Figure 6.

From Figures 5 and 6, it can be seen that there are what appear to be "hooks" near the points of maximum C_p for all span stations. This is a feature of the 3D boundary layer code, and is an indication that the code is functioning properly. To locate the attachment line, the code performs a series of iterations. These iterations take place around the maximum pressure location, which is the initial guess for the attachment line location. A feature in the code allows the user to choose the number of points before the maximum pressure location to use when iterating upon the location of the attachment line. For the NACA 0012 and the NACA 64A010, the number of points chosen was two. Figure 7, which is an enlargement of the attachment line region for certain span stations of the NACA 0012, shows that there are two points before the maximum pressure points. Such is also the case (although not shown here) for the NACA 64A010, which indicates the proper and expected functioning of the code to this point.

The 3D code also uses the reference cross sections (in subroutine 'refcr') for use in the attachment line location routine. The surface lengths are calculated from the reference cross sections, and the surface lengths are then used as independent variables in the interpolations for the attachment line relocation. For the NACA 0012, the output from subroutine 'refcr' is shown in Figure 8, while the output for the tapered NACA 64A010 is shown in Figure 9. Consistent with the taper of the NACA 64A010 and the fact that the trailing edge is at a constant X value of 1.0, the surface length "wedges" decrease in size as the tip of the wing is approached. For the NACA 0012, the "wedges" remain of constant size, but are merely displaced because of sweep. Figures 8 and 9 are consistent with Figures 1 and 2, because the results are entirely geometry dependent.

After quitting subroutine 'refcr', the code proceeds to subroutine 'reloc', which is the subroutine which performs the relocation procedure. After convergence is obtained for the attachment line, a spline interpolation for the pressure is performed. The pressures are calculated before statement 909 in subroutine 'reloc'. The result of this for the NACA 0012 is shown in Figure 10. The C_p plots at all spanwise locations are normalized to begin at an X of zero. As can be noted, the C_p plots at the various stations are quite similar, something already noted in Figure 5. Figure 11 shows the C_p plots in boundary layer coordinates. The X variable goes only to a value of approximately 0.6 because that is what was used in the original program. Higher values are possible. The same boundary layer X locations were also chosen for the tapered NACA 64A010.

The reason for the later difficulties with the code can be seen in Figure 12, which is a representative C_p plot for a particular spanwise location for the tapered NACA 64A010 airfoil. Although the C_p values have realistic magnitudes, the maximum value occurs far off the relocated attachment line (X of zero). Although not shown here, the relocated C_p values (in the program, the variables $xpt(i)$ and the corresponding $pbs(i,j)$ values near statement 909 in subroutine 'reloc') are unphysically high. Using such relocated and interpolated C_p distributions eventually causes an error in the code.

The reasons why the 3D code has difficulty using locally generated inputs to locate the attachment line is presently not known, although there are a variety of possibilities. There was not time in this work period for this author to correct the problem.

One of the possibilities is that the Cp profiles that are generated locally are not smooth enough for use by the 3D code. In the sample Test Case 10, the inviscid Hess code (the program used by V. Iyer to generate inviscid inputs for the NACA 0012, see Ref.4) was used to generate the pressure distribution, and then the resulting pressure distribution was put into the program int_wing/cor.f to eliminate the oscillations. The pressure distributions generated locally were not put into the smoothing program because it appeared that they were sufficiently smooth (see Figure 6). This may not be the case however.

It is also possible that difficulties arise because of the particular tapered nature of this version of the NACA 64A010 airfoil. To determine if this is the case would require yet a deeper immersion in the code, particularly into subroutine 'reloc', than was accomplished during the present work period.

b) PSX code of Th. Herbert

As reported in Ref.2, a 2D compressible code based on the Parabolized Stability Equations (PSE) was obtained from Th. Herbert of DynaFlow, Inc. This code is called the PSX code. During the current work period, this code was compiled on both Iris workstations and on EAGLE. Test cases for this code, provided earlier by Th. Herbert, were run to assure proper functioning of the code. The PSX code was then used extensively to run cases for comparison with a linear stability code (COMPOSE, Ref.5), and the results were presented to the APS at the DFD meeting in November, in Tallahassee, Florida (see section d).

c) PSE development

Development of an in-house stability code based upon the Parabolized Stability Equations was initiated in the previous work period, and continued into the present one. The author was notified in early January, 1993 that all further development of the code was to be cancelled, budget strictures being the reasons cited for the decision. Any work on the PSE which would be used at the FML was expected to be done by Th. Herbert of DynaFlow, Inc. of Columbus, Ohio under and SBIR, and possibly a doctoral student at the Arizona State University, Mr. T. Haynes.

d) APS paper

A paper entitled "Stability of Two-Dimensional Compressible Boundary Layers" was presented at the 45th Annual Meeting of the Division of Fluid Dynamics of the American Physical Society in Tallahassee, Florida on November 23, 1992 in Session FC: Compressible Boundary-Layer Instabilities. The abstract of the presentation is as follows:

Compressible Linear Stability Theory (LST) has been widely used for the prediction of the stability properties of high speed boundary layers. In conjunction with the eN method, LST has been widely used to compute transition location on geometries such as flat plates and cones. The Parabolized Stability Equation (PSE) method of Herbert and Bertolotti (Bull.

Am. Phys. Soc. ,Vol. 32, p. 2079, 1987) is a more recent procedure which promises to both duplicate the capabilities of LST as well as to go beyond it in predicting stability properties of boundary layers and transition locations. Using an LST code written by the author (documented in AEDC-TR-86-37, 1986), and a PSE code supplied by DynaFlow, Inc. (Th. Herbert, president), calculations for two-dimensional flat plate boundary layers are made for various supersonic Mach numbers. Comparisons are made between LST and PSE results to determine the limitations of LST as well as the advantages of the PSE method.

e) Annual Review of Fluid Mechanics paper

An article entitled "Results From Linear Stability Theory", co-authored with H. Reed of the Arizona State University, was initiated during this work period. The scope of the article is to address the contributions that linear stability theory has made to the knowledge and understanding that we now have in regard to the instability of boundary layers, with a focus on the elucidation of the physics of the processes which take place during instability. In particular, the agreement between linear stability theory as to unstable frequencies, the growth rates of those frequencies correlated with the Reynolds numbers, the most unstable modes, and the use of linear stability theory in conjunction with the eN method for the semi-empirical prediction of transition are to be a major focus of the work.

The topics to be covered are 2D and 3D flows, both incompressible and compressible. A brief overview of the article is provided here. We will begin with 2D flows first.

For 2D incompressible, the effect of suction, heating and cooling, and dp/dx are to be evaluated. In particular, for cones and flat plates, cooling stabilizes boundary layers and heating destabilizes. The effects of suction are generally considered to be stabilizing, as has been both postulated and demonstrated in a variety of ground and flight experiments. Yet some of the critical facets of suction are still not yet well known, such as required suction levels for various flowfields, and the order and distribution of the suction slots or holes. It is also known that suction can, under certain conditions, promote instabilities rather than provide a stabilizing influence.

One of the critical discoveries of linear stability theory is due to L. Mack of the Jet Propulsion Laboratory who discovered the existence of 2D modes (now named the Mack Modes) which first make their appearance in high supersonic or low hypersonic flowfields. For a flat plate, the most unstable modes are all in the streamwise direction up to a Mach number of approximately 0.8. At higher Mach numbers, the most unstable modes are oblique, ie. they travel in a direction which is not coincident with the streamwise direction. At a Mach number of approximately 4, a new mode, the Second Mode or the Mack Mode, with its own particular bandwidth of unstable frequencies and wavenumbers, makes its appearance. The growth rates for this mode are much higher than those for the First Mode, and instability growth is dominated by this mode. In addition to having high growth rates, it has been shown, both theoretically and experimentally, that this mode has some unexpected properties as well. For example, wall cooling has been observed to destabilize the boundary layer in Mack Mode dominated flowfields. This is the opposite of what occurs in First Mode dominated flows. Conversely, heating stabilizes the Mack Mode, and destabilizes the First Mode.

At higher hypersonic Mach numbers, equilibrium effects, as well as non-equilibrium effects become important, and so the assumption of a perfect gas cannot be used. Calculation of equilibrium gas effects, and non-equilibrium chemistry effects are not yet definitive, and experimental verification is extremely sparse, but the general findings seem to indicate a stabilizing effect upon the various flowfields that have been studied.

n 3D boundary layers, crossflow instabilities and attachment line instabilities must be considered in addition to the instabilities mentioned above. In particular, some of the important concerns are geometry and curvature, the oblique modes and how to properly calculate them, and the question as to whether the non-zero crossflow frequencies are more unstable than the traveling waves.

Because of the time demands upon both of the authors, the Annual Review of Fluid Mechanics article was not prepared in time for inclusion in the 1994 volume, but it will be completed for inclusion in the subsequent volume.

f) Other activities

During this work period, various COSAL calculations using mean flow parameters provided by E. Tu of NASA Ames were made for the F16XL Ship 2. Both crossflow calculations and TS (Tollmien-Schlichting) calculations were made as routine continuing support.

REFERENCES

- 1) Iyer, V., "Computation of Three-Dimensional Compressible Boundary Layers to Fourth-Order Accuracy on Wings and Fuselages", NASA Contractor Report 4269, 1990.
- 2) Gasperas, G., "High Speed Transition Prediction", MCAT Institute Progress Report 92-017, September, 1992.
- 3) Malik, M. R., "COSAL--A black-box compressible stability analysis code for transition prediction in three-dimesnional boundarylayers", NASA Contractor Report 165925, May, 1982
- 4) Hess, J.L., "Calculation of Potential Flow About Arbitrary Three-Dimensional Lifting Bodies," Report MDC J5679/01 (Contract N00019-C-71-0524), Douglas Aircraft Co., October 1972 (available from DTIC as AD 755 480).
- 5) Gasperas, G., "COMPOSE; A Program for the Solution of the Compressible Linearized Two-Dimensional Boundary-Layer Stability Equations, User's Manual", AEDC-TR-86-37, 1986.

NACA 0012, 20 degrees sweep

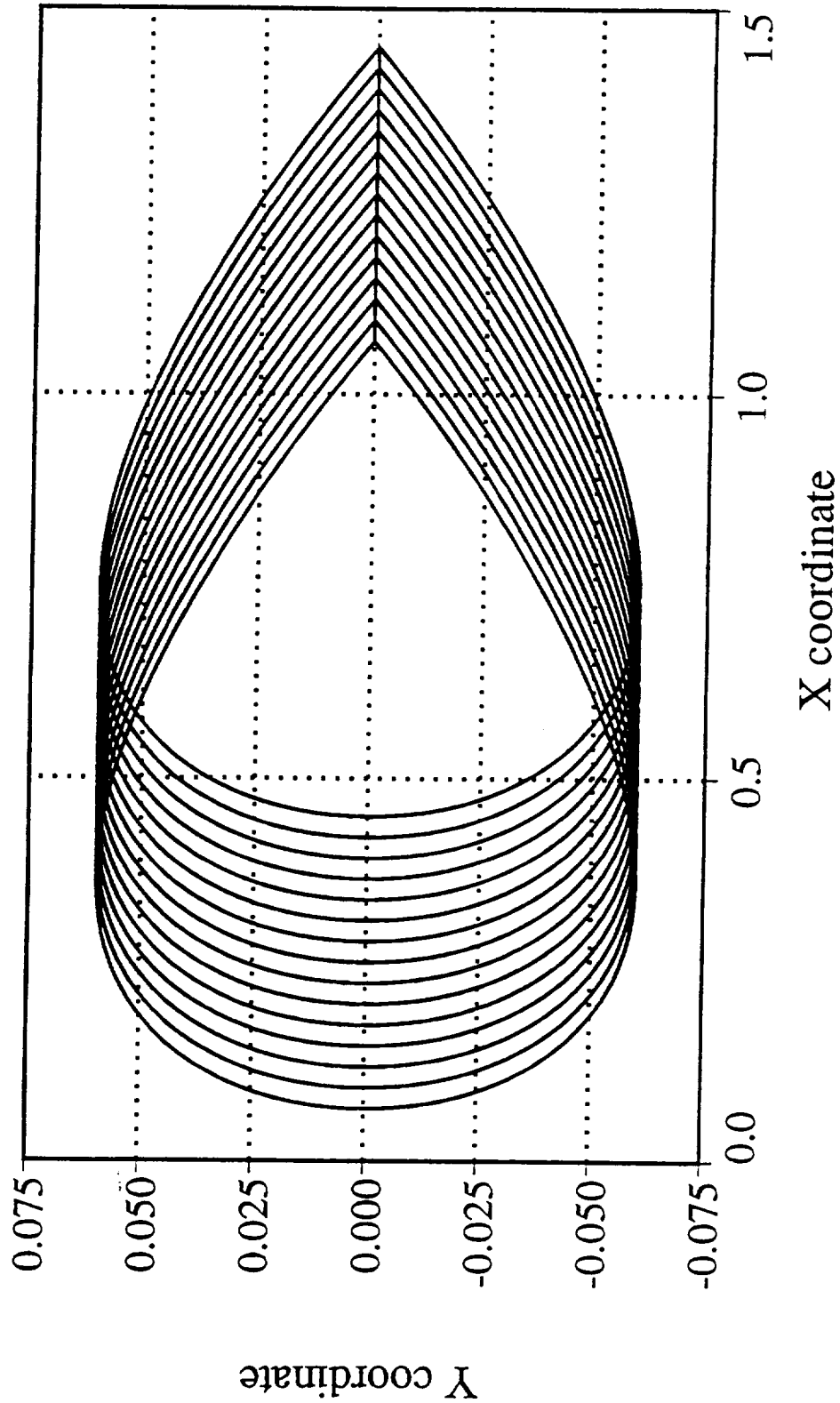


Figure 1.

NACA 0012 Airfoil Geometry Definition

Tapered NACA 64A010, 45 degrees sweep

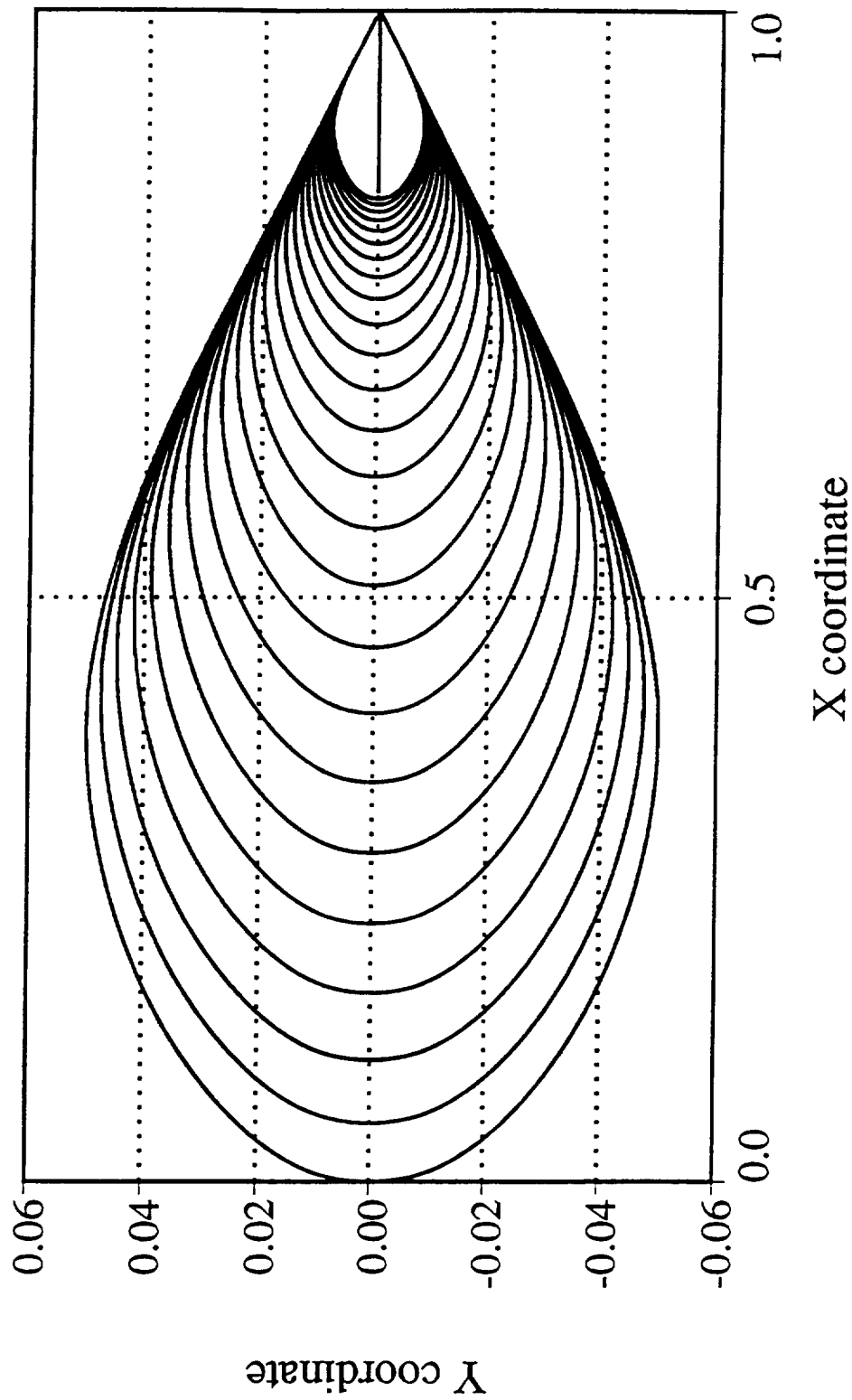


Figure 2.

NACA 64A010 Geometry Definition

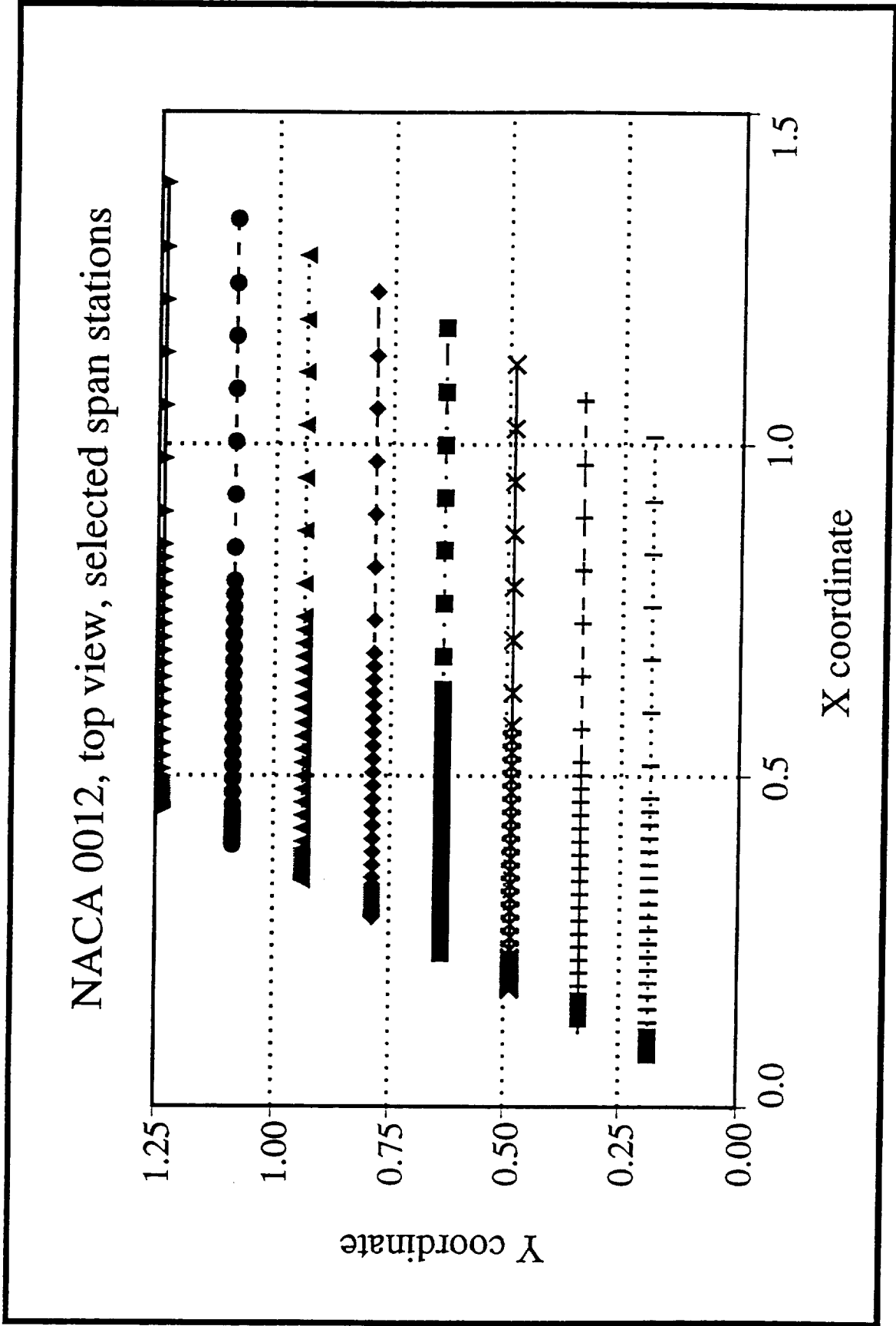


Figure 3.

NACA 0012 Top view, selected span stations

Tapered NACA 64A010, top view, selected stations

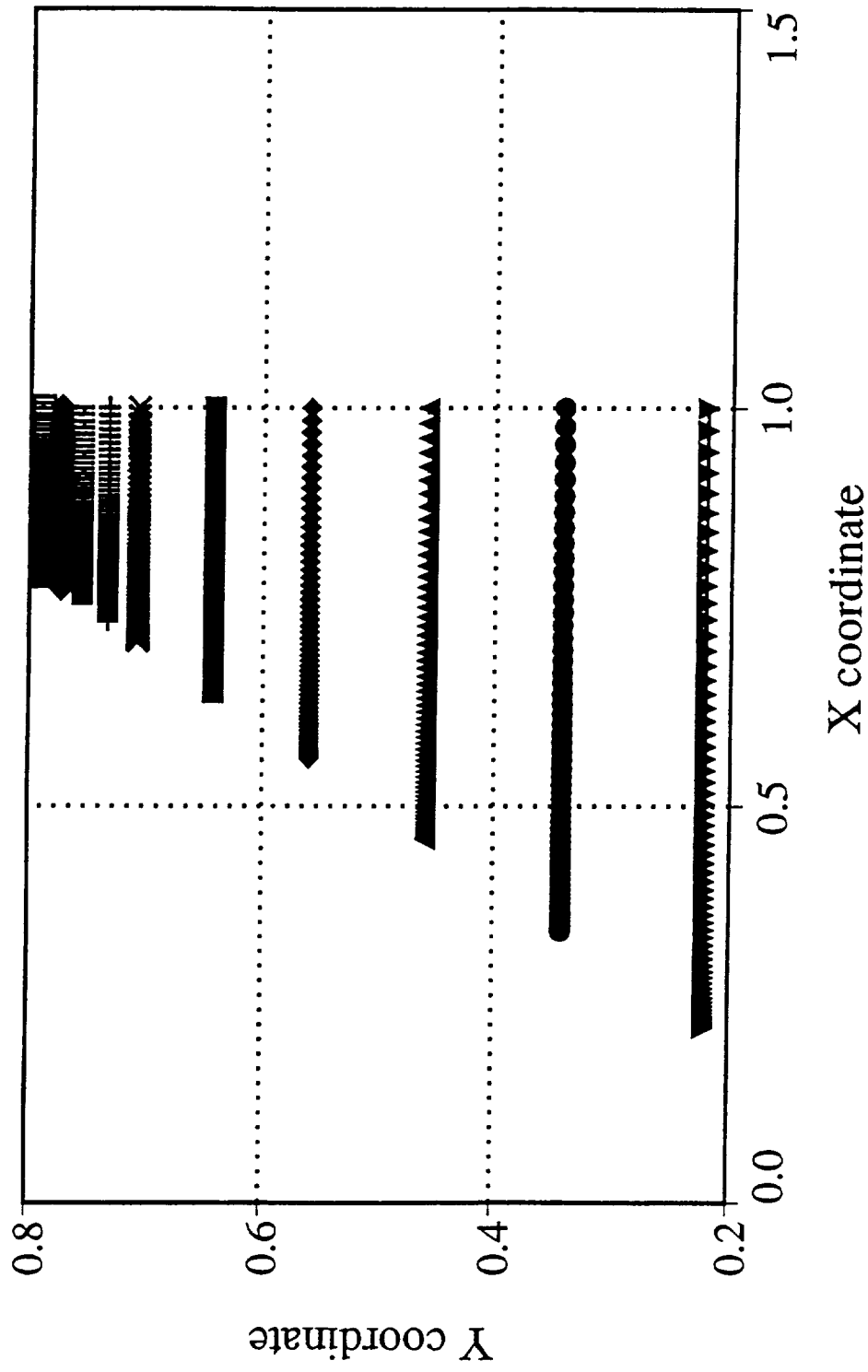


Figure 4.

Tapered NACA 64A010 Top view, selected span stations

NACA 0012, Cp plots, various span stations

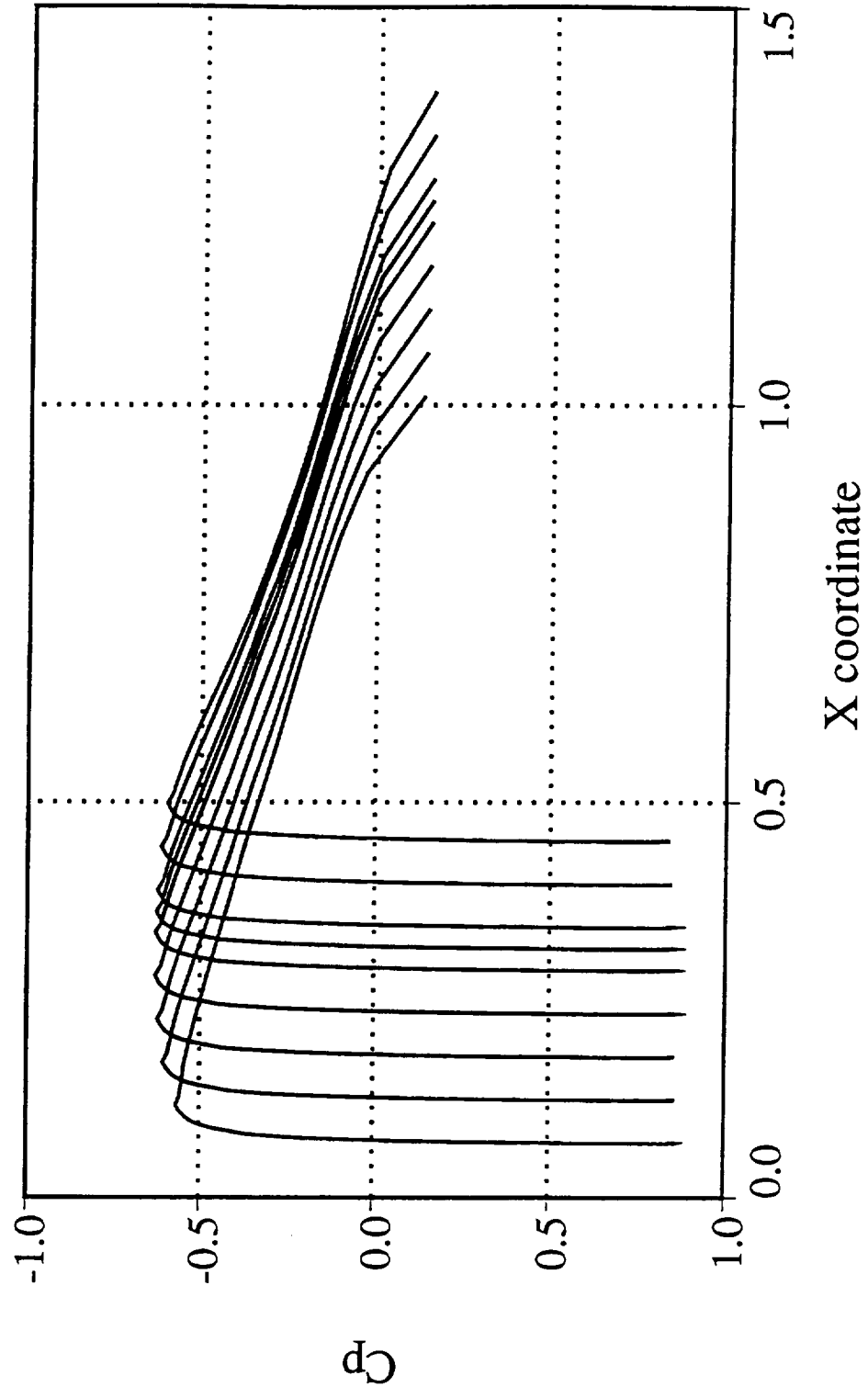


Figure 5.

NACA 0012 Selected Cp plots

NACA 64A010, Cp plots, various span stations

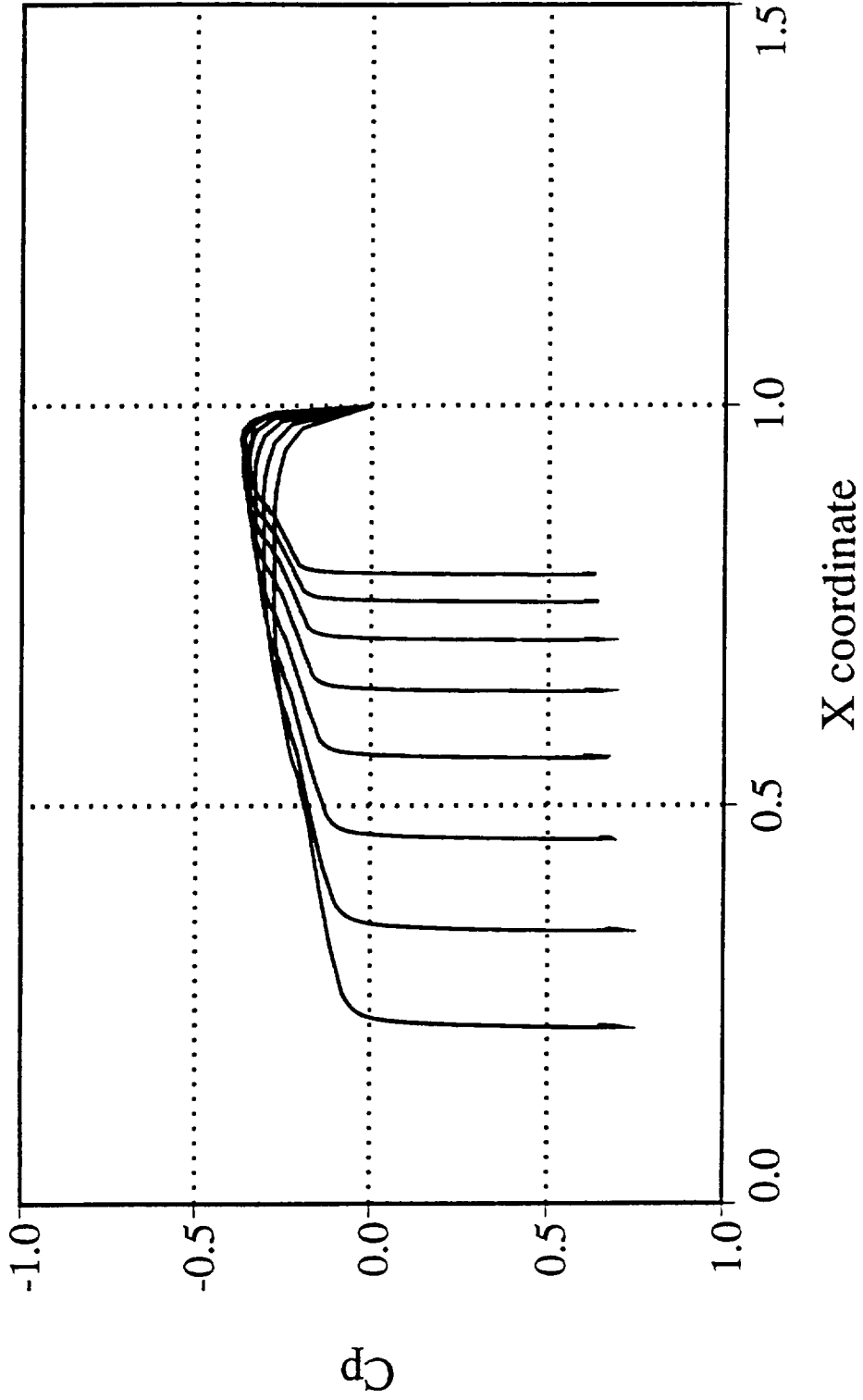


Figure 6.

NACA 64A010 Selected Cp plots

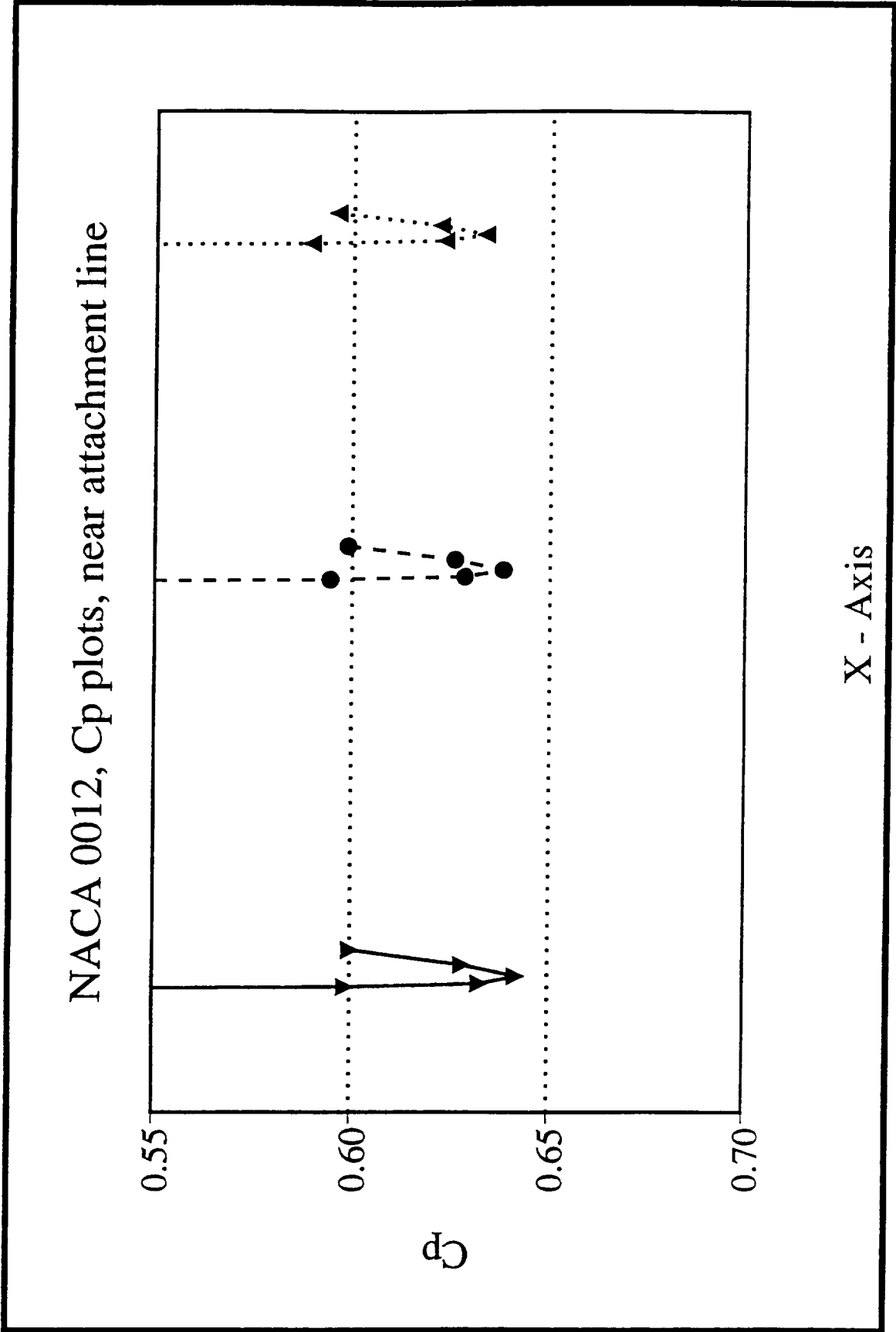


Figure 7.

NACA 0012, selected reference cross sections

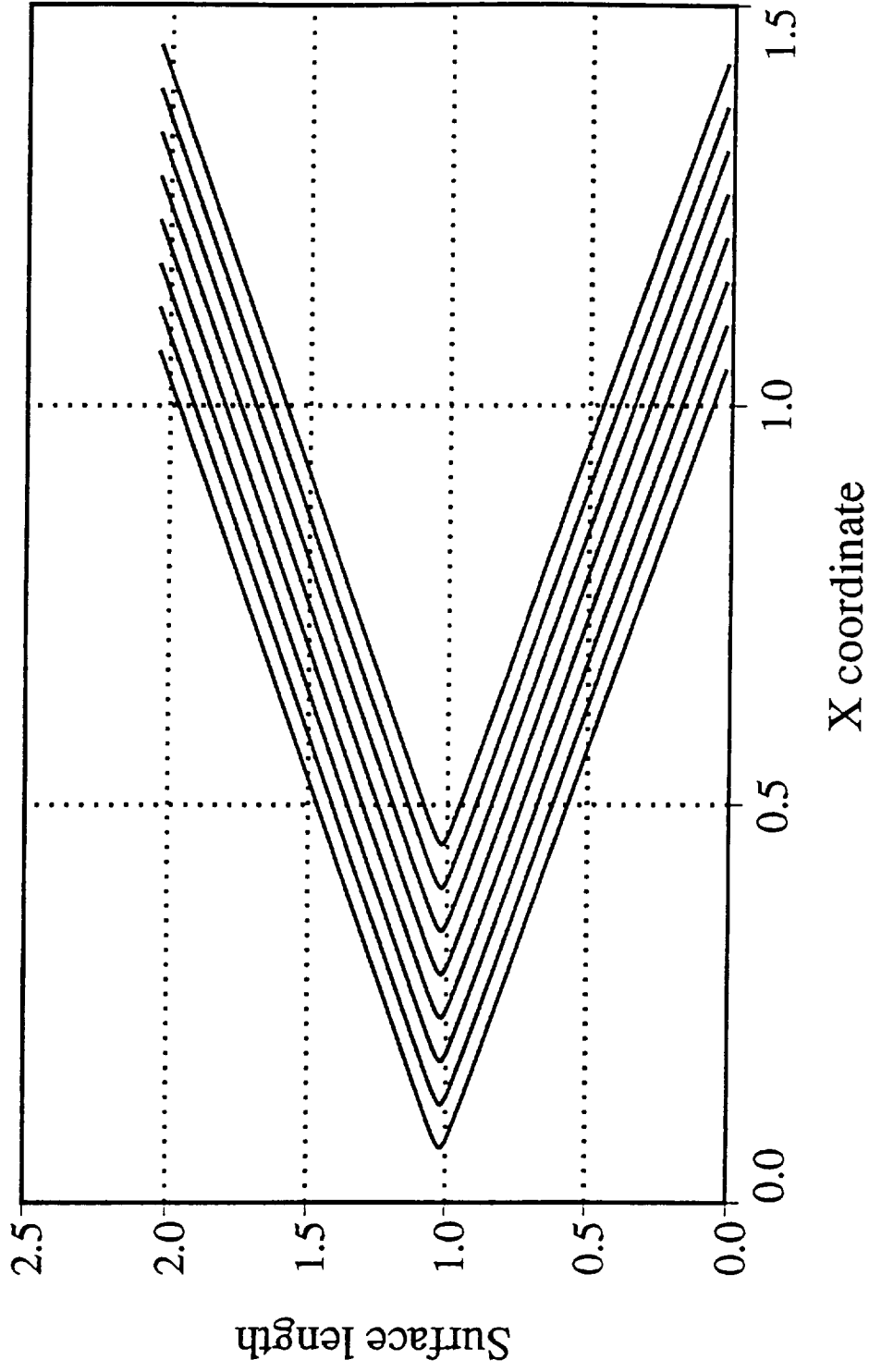


Figure 8.

NACA 0012 Surface Length Distribution

Tapered NACA 64A010, reference cross sections

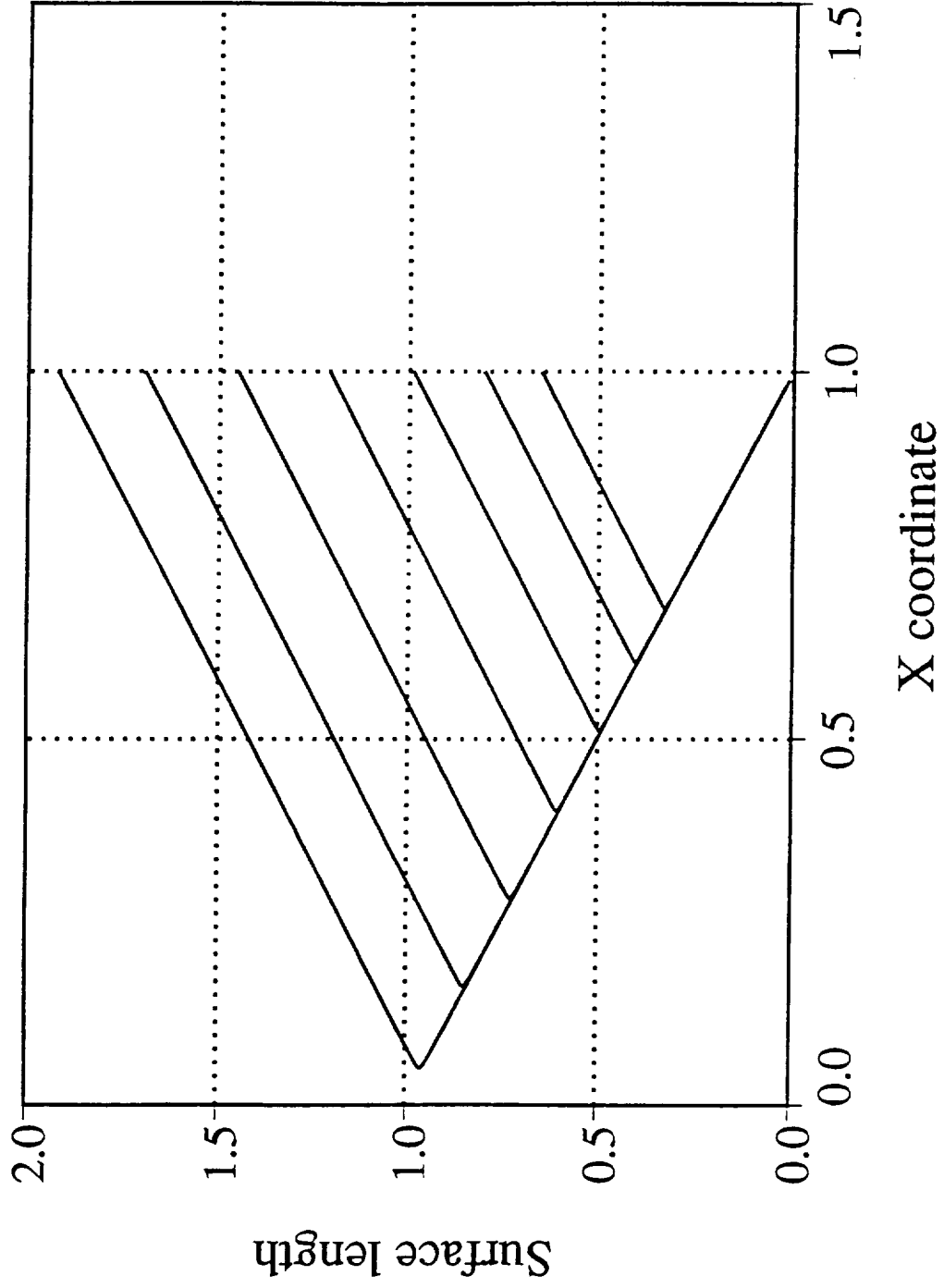


Figure 9.

Tapered NACA 64A010 Surface Length Distribution

NACA 0012, Cp's after relocation procedure

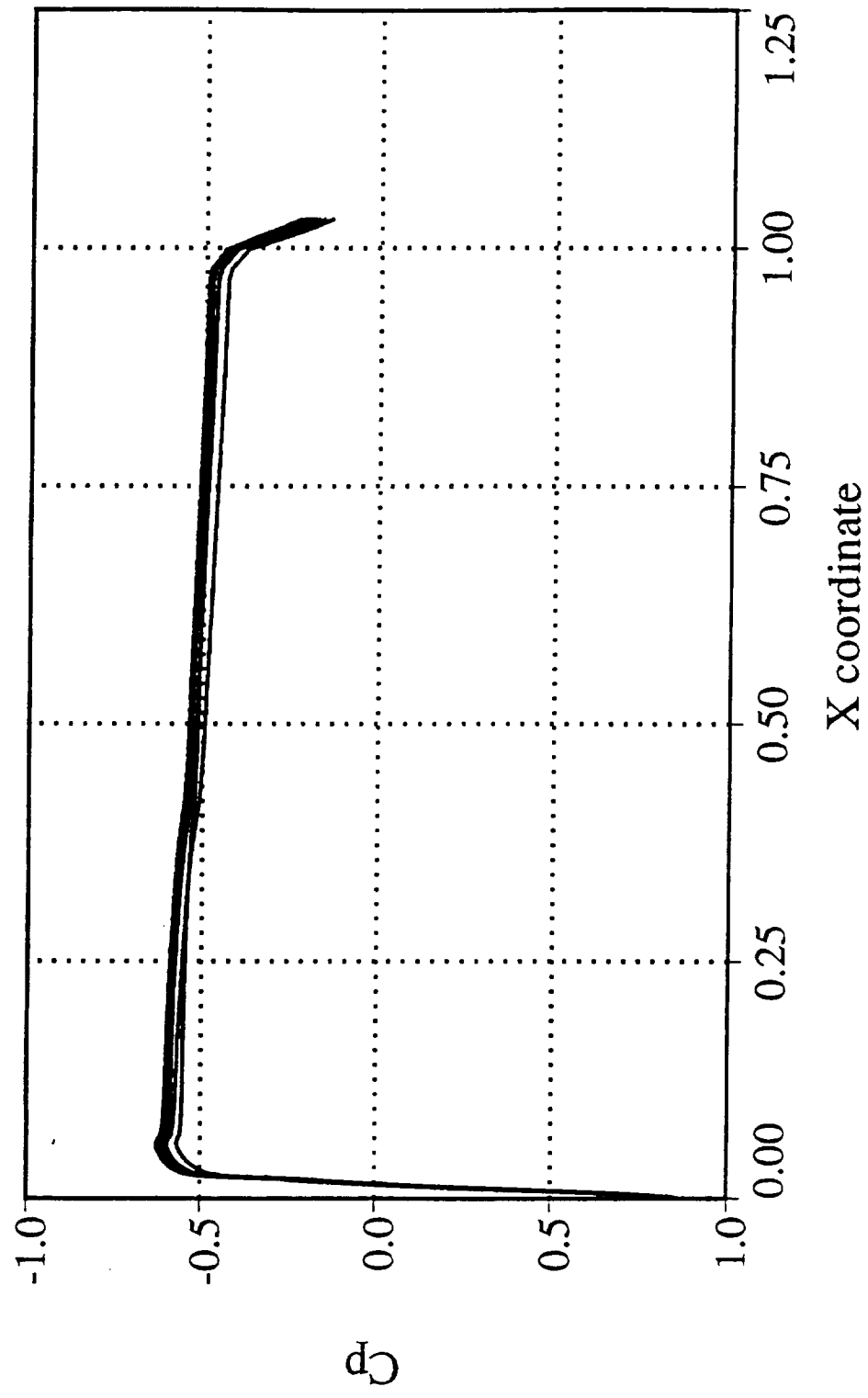


Figure 10.

NACA 0012 Cp distribution after relocation

NACA 0012, after relocation procedure

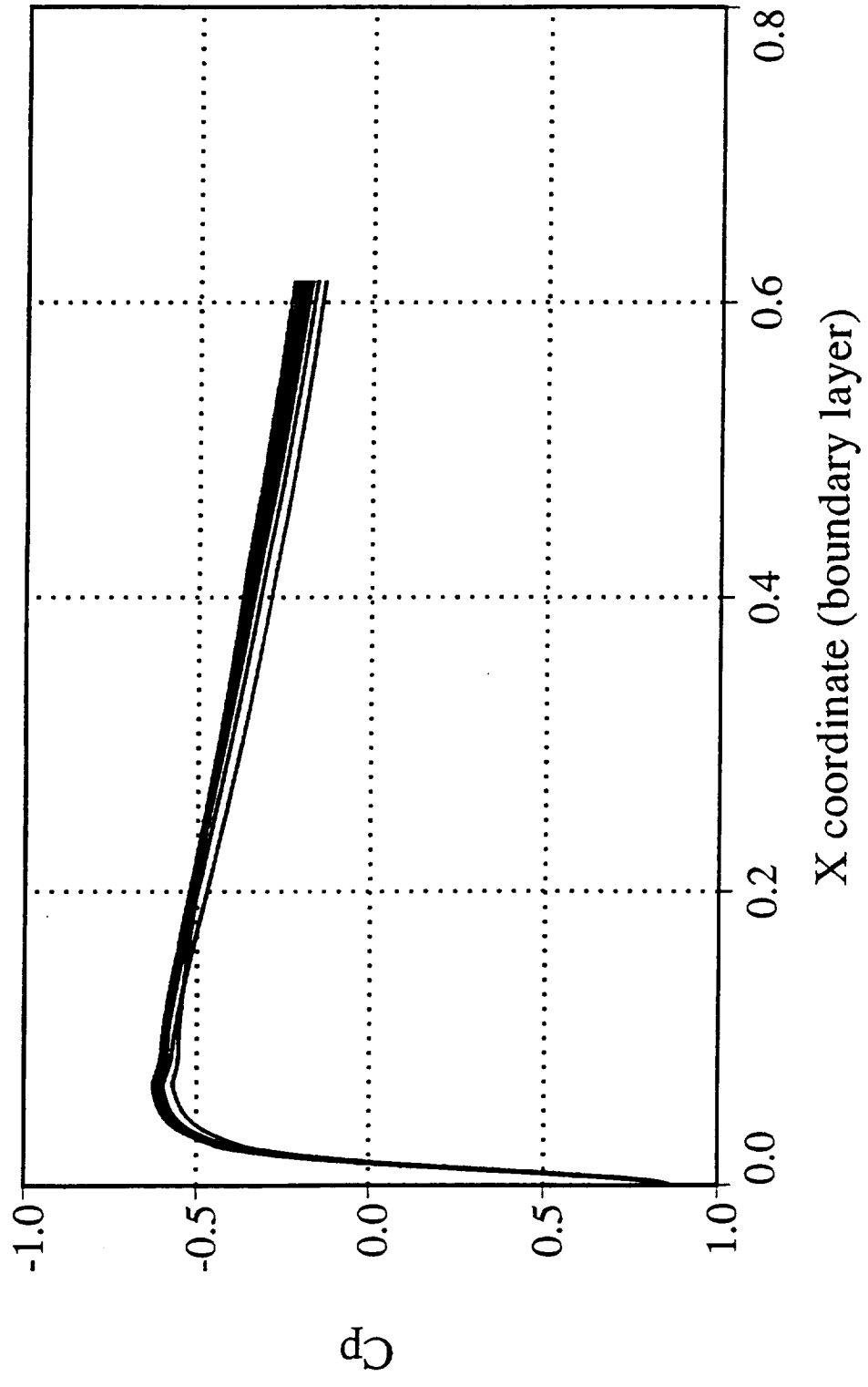


Figure 11.

NACA 0012 C_p distribution in boundary layer

Tapered NACA 64A010, Cp after relocation

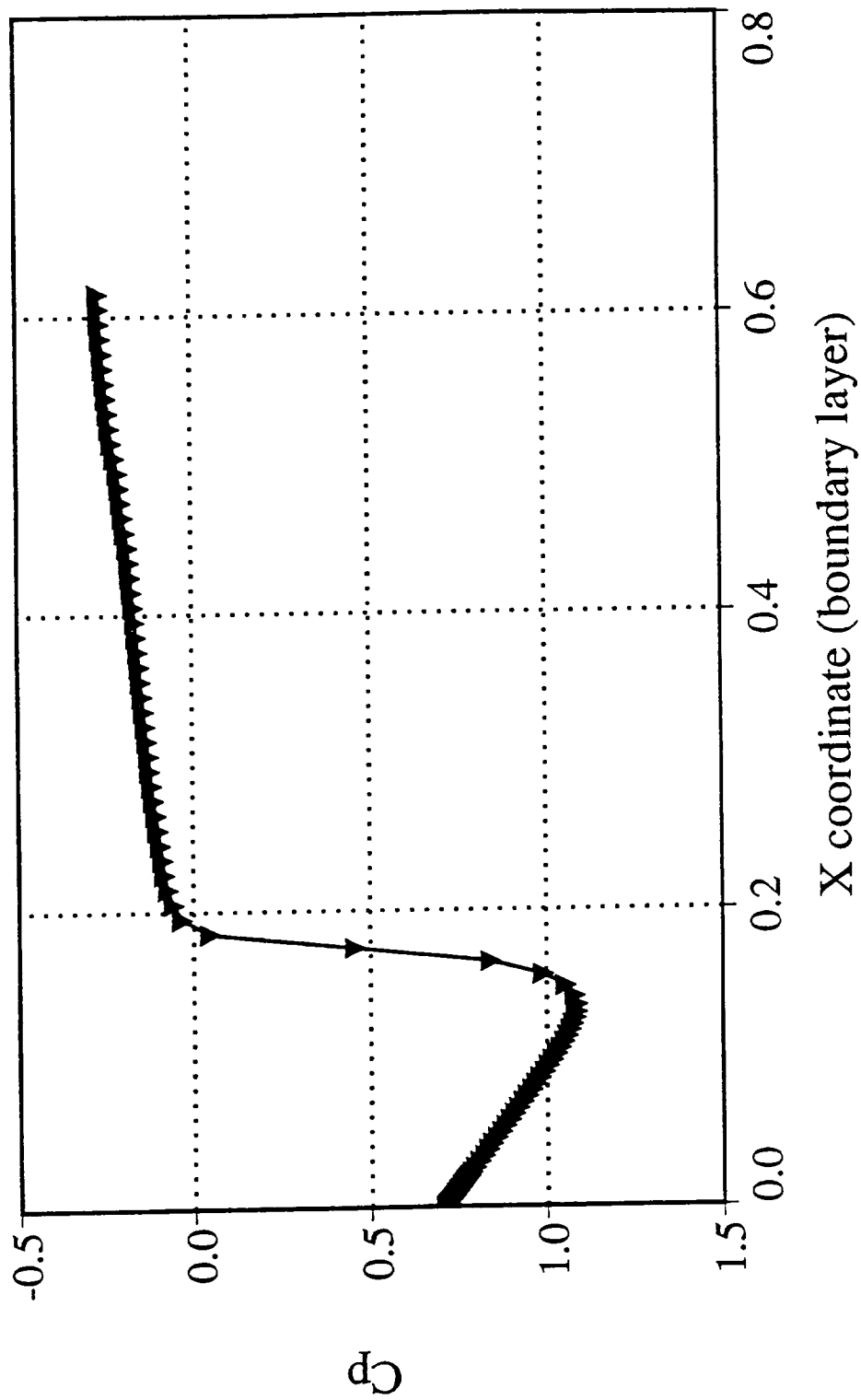


Figure 12.

Tapered NACA 64A010 C_p distribution after relocation